Simulations and analysis of PACS Spectrometer Ramps under irradiation conditions: impact on science goals and AOT design

Martin Groenewegen (ICC KUL)

DOCUMENT CHANGE RECORD

Version	Date	Changes	Remarks
Draft 0	05-April-2006	–	started new document
Draft 1	28-July-2006		Released to ICC

Reference Documents

RD 1 – Test Plan and procedure for investigation of glitch event rate and collected charge variation in the Ge:Ga detectors during proton irradiation at UCL-CRC, PACS-ME-TP-009, (issue 1.2, 10 March 2004), (issue 2.2, 5 May 2005), (issue 3.1, 2 October 2005), Katterloher, Barl & Schubert
RD 2 – Analysis of the April 2005 proton test data, PICC-KL-TN-020, M.A.T. Groenewegen & P. Royer
RD 3 – Analysis of the October 2005 proton test data on the low-stress module, PICC-KL-TN-024, M.A.T. Groenewegen
RD 4 – UCL-CRC Proton tests of March 2004: glitch height distribution, PICC-KL-TN-012, M.A.T. Groenewegen (KUL)
RD 5 – FM proton irradiation test. Flasher sequences, PICC-KL-TN-021, P. Royer, 8 Dec. 2005
RD 6 – FM proton irradiation test. High & Low stress modules I: Glitch effects and curing, PICC-KL-TN-022, P. Royer, 11 Jan. 2006
RD 7 – CQM Proton Irradiation Test Analysis,PICC-KL-TN-011, draft 2, P. Royer, 3 Jan. 2005
RD 8 – Testing Glitch Detection Algorithms by Monte-Carlo Simulations, PICC-KL-TN-019, M.A.T. Groenewegen, P. Royer, J. Schreiber, A. Baier
RD 9 – Simulations of Galactic Cosmic Ray impacts into the Herschel Photodetector array camera and spectrometer (PACS) with the GEANT 4 code, Christian Bongardo, Ph.D. thesis, Padova University, 2 Jan. 2006
RD 10 – Fitting PACS ramps with analytical models. Part III: The IMEC model, PICC-KL-TN-010, M.A.T. Groenewegen & P. Merken
RD 11 – ISO/FIRST glitches working group Final Report, SAI/2001-013/Rp, issue 1.1, 21 august 2001, Heras (Editor)

1. Introduction

Following the proton irradiation tests which took place in the cyclotron at Louvain-La-Neuve (UCL-CRC) in March 2004, April 2005 and October 2005 (described in issues 1.2, 2.2 and 3.1 of RD 1, respectively) there has been a series of reports on the analysis of this data focusing on the noise properties and S/N aspects of the pre-beam data (RD 2, RD 3), glitch rate (RD 2-4), curing (RD 5), responsivity drifts (RD 6, RD 7), and glitch detection algorithms (RD 8).

The reports only considered the raw ramps generated during the tests, while in-flight the on-board processing will generate raw ramps for selected pixels only, and the default output will be averages over 4, 8, or 16 consecutive non-destructive readouts (NDRs), or slope fitting, depending on issues like CPU capacity and data compression efficiency.

Another aspect not yet considered is the fact that the radiation effect in L2 will be different from that in the cyclotron. The work in RD 9, that simulated the radiation environment in the cyclotron and in L2, suggests that in space there will be more events but with less energy that in the UCL-CRC tests.

In this document we will consider two radiation environments:

(A) The glitch rate and distribution of deposited energy as derived from the glitch height distribution observed in the UCL-CRC tests, and,

(B) The theoretically predicted glitch rate and energy distribution in L2 at the crystal surface, scaled in two different ways to give the deposited energy distribution in the crystal.

These glitches will be added to ramps that may be thought of as representative, namely in case (A) ramps observed at the responsivity plateau of the October 2005 tests (assuming a case where there will be no or infrequent curing), and (B) ramps observed without radiation (assuming here that the less energetic impacts predicted in L2 will not lead to drastic changes in responsivity).

Finally, raw ramps and averages over 4, 8, 16 NDRs are generated, and then analysed. The other option of the onboard processing software is also considered, namely slope fitting [to the raw ramp without deglitching].

The analysis will take into account glitch detection and slope fitting to the remainder of the ramp. One of the simulated detectors will have a slightly different signal to be possible to compare 'on-source' with 'off-source' and verify if this signal can be detected.

2. Generation of ramps

The ramps are generated with the IMEC model of the ramps, as described in RD 10.

To recall, the ramps are described as:

$$V(t) = V(0) + A\ \ (-1.0 + \exp(-t\ \zeta\ \omega) \times (\cosh(t\ \omega\ d) + (\zeta + \omega\ \tau)/d \times \sinh(t\ \omega\ d))) \tag{1}$$

with

$$d = \sqrt{\zeta^2 - 1}$$

where t represent time, and ω and ζ are known via the relations

$$\omega = 1.0/\sqrt{(C_{\rm f} + C_{\rm p})\ R_{\rm d}\ \tau_{\rm c}} \tag{2}$$

and

$$\zeta = \omega \times \frac{1}{2}\left(((1.0 + A)\ C_{\rm f} + C_{\rm p})\ R_{\rm d} + \tau_{\rm c}\right) \tag{3}$$

The parameters of the model are therefore:

$V(0)$, Voltage at first read-out
A, amplifier gain
$C_{\rm f}$, feedback capacitance
$C_{\rm p}$, parasitic capacitance
$R_{\rm d}$, resistance of the detector, a proxy for the power of the in-falling infra-red light
$\tau_{\rm c}$, time constant of the amplifier
τ, ad-hoc parameter, related to the “bump”
$V_{\rm b}$, bias voltage

It is also useful to define a *slope* (in units of V/s), as in the limit of infinite gain Equation (1) becomes

$$slope = \frac{dV(t)}{dt} = \frac{-V_{\rm b}}{C_{\rm f}\ R_{\rm d}} \tag{4}$$

In other words, a *slope* is adopted and $R_{\rm d}$ is calculated according to Eq. 4 and then used in the generation of the ramps.

The feedback capacitance and bias value are known quantities.

Compared to the 2003 MPE six-pack tests the ramps seen during the UCL-CRC test show almost no ‘bump”. Therefore it is decided to fix τ to zero.

A, $C_{\rm p}$ and $\tau_{\rm c}$ are kept at the values derived in RD 2. These values are A = 150, $C_{\rm p}$ = 2.0 pF, $\tau_{\rm c}$ = 0.06. $V(0)$ is arbitrarily set at 2.0 V.

Using these results the simulated ramps are generated.

3. Proton energy distribution

The distribution function of the deposited energy of the particles is described by a Landau function (2 parameters, a mean energy, E_p and a 'shape' parameter, R, see RD 4 and below), where the probability density function is given by:

$$F(x) = \frac{1}{\sqrt{2\pi}} \exp(-0.5\ (x + \exp(-x))) \tag{5}$$

x is related to the energy E, most probable energy E_p and a material constant R, via,

$$x = R\ (E - E_{\rm p}) \tag{6}$$

The formalism to convert the deposited energy to the jump in voltage is taken from RD 4, RD 11.

$$\Delta V[\mathrm{Volt}] = 0.1986\ \Delta E(\mathrm{MeV})\ \frac{R[\mathrm{A/W}]}{c_{\rm f}[\mathrm{pF}]\ \eta\ \lambda[\mu\mathrm{m}]\ E_{\rm g}[\mathrm{eV}]} \tag{7}$$

which for $E_{\rm g}$ the energy loss per electron-hole pair produced (2.9 eV for Ge:GA), η is the quantum efficiency (taken to be 0.3, Poglitsch, private communication) and for the tests with the un-stressed module (wavelength of 110 μm) can be written as:

$$\Delta V[\mathrm{Volt}] = 2.08\ \Delta E(\mathrm{MeV})\ \frac{dV}{dt}[\mathrm{V/s}]/P[10^{-15}\mathrm{W}] \equiv \mathrm{CF}\ \Delta E(\mathrm{MeV}) \tag{8}$$

where CF, a *Conversion Factor* is introduced.

Finally the particle flux (in /cm^2/s), pFlux, is a parameter. The pixels are assumed to be of size 1mm x 1.5mm.

The generation of the ramps proceeds as follows:

- The "perfect" ramp is generated according to the parameters for the IMEC model, resulting in **VoltN**. One important issue here is that *slope* is allowed to vary linearly in time to simulate the continuing change in overall responsivity during irradiation.
- Integrating noise is considered by looping over the NDRs and calculating:

  Volt[k] = Volt[k-1]+ (VoltN[k]-VoltN[k-1])* (poisson(Nelectrons) / Nelectrons)

  where poisson(Nelectrons) represents the draw of a Poissonian distribution with number Nelectrons.

  Nelectrons is calculated from:

  $$N_{\rm electrons} = (V_{\rm b}/R_{\rm d})/1.602\,10^{-19}/256./fudge, \tag{9}$$

  which represents the number of electrons reaching the capacitor per NDR, corrected by a fudge factor, tuned to get the observed integrating noise value. The fact that the derived values for *fudge* are larger than unity implies that the integrating noise is larger than expected.
- Gaussian post-integration noise is added at every NDR.
- A loop over the NDRs is started. A random number is generated. If it is smaller than (pFlux / 256 * 0.015) there is a glitch.

  In that case, an energy is randomly drawn from the Landau distribution, and the glitch height is determined using the appropriate factor, CF. The location of the glitch (ramp, detector, NDR) and voltage jump are saved to file. The Voltages at the current NDR and after are lowered by the calculated voltage jump, then the next NDR is considered.
- The raw ramps, the averages of 4, 8, 16 NDR, and the slope fitted to the raw ramps are written to an IA saveset.

4. Data sets generated

Data sets represetative for the low-stress modules ($\lambda \lesssim 110 \mu m$) for two radiation environments are generated:

- Representative of the UCL-CRC tests in October 2005.

  In particular data taken at the "responsivity plateau" at the end of the test which showed that the best S/N is reached for relatively low bias and short ramp length[1].

  In particular we take the data for detector 3 of file T25b120t025c14n256_#L_115, with Bias= 120 mV, Capacitor= 1.42 pF, ramplength 0.25s, and assumed infalling power of 1.3 10^{-14} W (RD 1).

  We derived a *slope* of -0.9916 V/s with a standard deviation of 0.0409 when considering the 256 ramps in that file. For that configuration the conversion factor from proton energy to glitch (Eq. 8) is CF= 0.16.

  From pre-irradiation data an post-integration noise of 102. E(-5) V is found for a capacitance of 1.4 pF, and for that slope an integration noise of 275. E(-6) V is expected (RD 3).

  From the observed behaviour of the noise as a function of read-out it is derived that even at the responsivity "plateau" the responsivity change is 0.0004 of the *slope* every 1/4s (Figure 1), and this value is adopted in the simulation.

  Analysis of the glitches showed that the flux was pFlux= 16 ($s^{-1}cm^{-2}$), and the deposited energy distribution can be described by a Landau function with most probable energy $E_{\rm p}$= 0.1 MeV, and material constant R= 10.

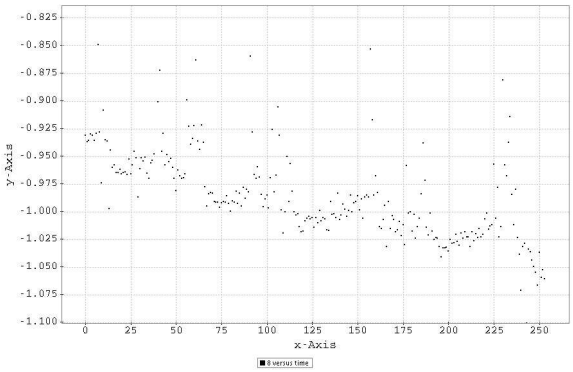

Figure 1: Signal (V/s) versus ramp number in the file T25b120t025c14n256_#L_115 at the "responsivity plateau". The signal still changes at a small level.

- Representative of L2 environment.

  As the effect of irradiation may be smaller in L2 than in the cyclotron test (see below) the detector setting are chosen such that they give the best S/N in the pre-irradiation conditions, i.e. large bias and small capacitor value.

  In particular we take the data for detector 3 of file T25b200t025c04n256_#N_3, with Bias= 200 mV, Capacitor= 0.41 pF, ramplength 0.25s, and assumed infalling power of 1.3 10^{-14} W (RD 1).

  We derived a *slope* of -0.8333 V/s with a standard deviation of 0.0048 when considering the 256 ramps in that file. For that configuration the conversion factor from proton energy to glitch is CF= 0.13. A post-integration noise of 182 E(-5) V and an integration noise of 189 E(-6) V were found (RD 3). This implies *fudge*= 29.

  As an illustration how well the noise properties can be simulated, Figure 2 shows the measured (left) and simulated (right) noise as a function of readout.

[1] Pre-beam data also showed a better S/N for lower capacitor values, but the data at the responsivity plateau was all taken at 1.4 pF.

RD 9 presents the predicted energy distribution at the crystal surface for the conditions in L2 for a solar minimum and a solar maximum. It can be described in both cases by a Landau distribution with $E_{\rm p}$= 0.01 MeV and R= 8, with a glitch rate of, respectively, pFlux= 120 and 60 ($s^{-1}cm^{-2}$).

From the simulations of the UCL-CRC tests by the same group we know that the predicted energy at the crystal surface is in agreement with independent calculations, and that the predicted glitch rate is to better than a factor of 2 in agreement with what is actually observed in the tests, but also that the deposited energy is significantly smaller that that at the crystal surface, by about a factor of 100 (typically from 10 MeV at the crystal surface to 0.1 MeV deposited).

Therefore the deposited energy distribution will be described by a Landau distribution with $E_{\rm p}$= 0.0001 MeV and R= 8, and assuming high event rate of 120 ($s^{-1}cm^{-2}$) corresponding to the solar minimum.

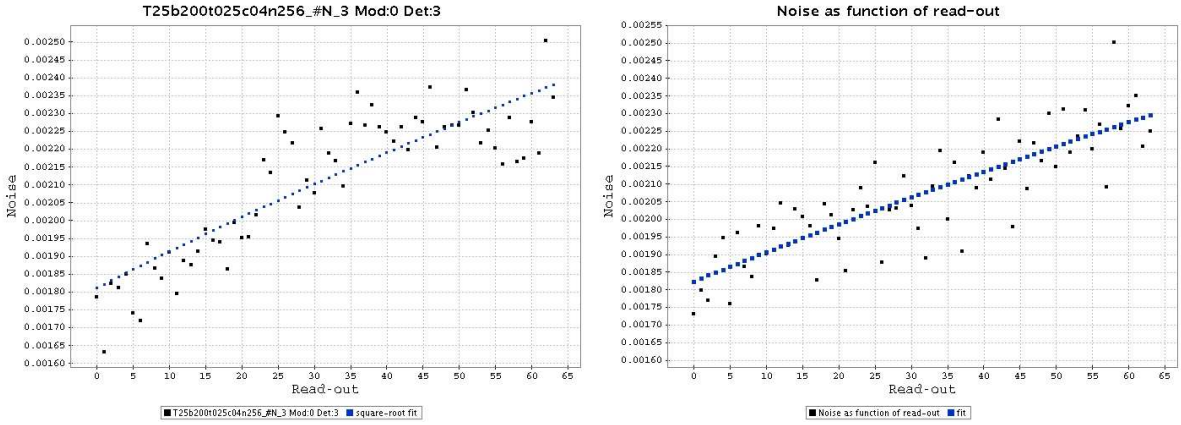

Figure 2: Noise (V) as a function of readout for the 256 ramps in file T25b200t025c04n256_#N_3. Left the actual observation, on the right the result of the simulation. The blue line is a fit of the form: $\sigma^2 = (\sigma_p)^2 + j\ (\sigma_i)^2$ as a function of read-out j, where σ_p and σ_i are the post-integration and integration noise, respectively.

For the high-stress modules ($\lambda \gtrsim 110 \mu m$) one dataset is generated:

- Representative of the L2 environment, based on the UCL-CRC tests in April 2005.

  Again a file with ramplength of 1/4s was taken that gave the best S/N in the pre-irradiation conditions.

  In particular we take the data for detector 3 of file T185b70d10t025c02n256_#N_3, with Bias= 70 mV, Capacitor= 0.23 pF, ramplength 0.25s, and assumed infalling power of 1.7 10^{-15} W (RD 1).

  We derived a *slope* of -0.6046 V/s with a standard deviation of 0.0045 when considering the 256 ramps in that file. For that configuration the conversion factor from proton energy to glitch is CF= 0.48. A post-integration noise of 249 E(-5) V and an integration noise of 160 E(-6) V were found (RD 2). This implies *fudge*= 16.

  As before, the deposited energy distribution will be described by a Landau distribution with $E_{\rm p}$= 0.0001 MeV and R= 8, and assuming high event rate of pFlux= 120 ($s^{-1}cm^{-2}$) corresponding to the solar minimum.

  As an alternative, the case of $E_{\rm p}$= 0.01 MeV and R= 8 but with CF= 0.0048, is also considered. The difference to the standard description is that shape of the energy distribution at the crystal surface is kept but the deposited energies are 1% of that, while in the standard description the mean deposited energy is set at 1% of the mean energy at the crystal surface but the parameter describing the shape of the distribution is the same.

Additional parameters are: nRamp (the number of ramps generated) for each of nDet (number of detectors; here 16). Each ramp has nNDR read-outs (here 64 or 32).

5. AOT design

The analysis of the simulated ramps are geared towards 2 important AOTs:

- Line Scan, and Range Scan at highest sampling density

  -2 ramps of 1/4s per chopper plateau
  -2 chopper plateaus per chopper cycle
  -1 chopper cycle
  -16 pixels stepped at 1/3 pixel
  -up-and-down scan
  -1 nod cycle

  This implies that 384 ramps see one line.

- Range Scan, and SED Mode at Nyquist sampling

  -2 ramps of 1/8s per chopper plateau
  -2 chopper plateaus per chopper cycle
  -2 chopper cycles
  -every line in seen by 2 pixels
  -up-and-down scan
  -1 nod cycle

  This implies that 32 ramps see one line.

  In SED mode it is foreseen to do (A) a full grating scan in third order (55 - 72 μm in 210 steps), obtaining in parallel data in first order between 165 and 210 μm, followed by (B) a full grating scan in first order (105 - 210 μm in 360 steps), obtaining in parallel data in second order between 72 and 105 μm.

  A full PACS scan taken in this way will take about 40 minutes.

6. Glitch detection optimisation

Two glitch detection methods are employed. The default one is based on the statistical Q-test, as implemented by Pierre Royer (and available as SPG module named SPG_RampDeglitch.py).

In this implementations two 'contrast' functions are computed based on differential ramps, (s[i+1]-s[i]) and (s[i+2]-s[i]). Parameters are, for each contrast function, a threshold and a number of high and low outliers to be removed when calculating the range in the contrast.

However, this algorithm does not work when the number of available data is too few, like with 1/4s ramps and averaging over 16 NDRs and 1/8s with averaging over 8 NDRs (only 4 sub-ramps are available).

For this reason a very simple edge detection is employed in these cases, solely for the purpose of this document, which is outlined in the Appendix for completeness.

In a first step the parameters for glitch detection were optimised in the following way:

- The equivalent of a few minutes of data was generated (e.g. 3600 ramps of $1/4s$) in order to have sufficient statistics on the number of glitches.
- For the raw ramps we set: n_low1=1, n_high1=1, n_low2=2, n_high2=2

  For the averages over 4, 8 and 16 NDRs we set: n_low1=0, n_high1=0, n_low2=0, n_high2=0

  For the ramps of 1/4 and 1/8s and averages over 16 NDRs the simple edge detection algorithm is applied. For the 1/8s ramps with averaging over 16 NDRs no deglitching on a ramp can be applied, as there are only two sub-ramps available per ramp.

  The statements above imply that deglitching is attempted on single ramps. No attempts have been made to use temporal, spatial or spectral redundant information.
- As recommended by PR we always use threshold2= $\frac{1}{2}$ threshold1 for his algorithm.
- *threshold1* is then determined to give 2% false detections. As the sub-ramps beyond a glitch are not used in the slope fitting it is important to have a small fraction of false detections.

Table 1 lists the percentage of glitches recovered allowing for at most 2% false detections. A few conclusions can be drawn. The larger the number of available points per ramp, the better the statistics and the higher the recovery rate: both averaging ramps, or shorter ramps will lead to lesser detection rates. With the current scheme of averaging over 16 NDRs at most 30% of the glitches may be recovered. In the description where all particles deposit only 1% of their energy, deglitching is no longer effective (last part of Table 1).

Table 1: Percentage of glitches recovered, allowing 2% false detections. Numbers between parenthesis are based on a very simple edge-detection algorithm outlined in the Appendix, the others are based on PR Q-test. Top part of the table is for the low-stress module, middle and bottom part for high-stress module, with middle panel for a mean energy of 0.0001 MeV and CF = 0.48, while bottom panel is for mean energy of 0.01 MeV and CF = 0.0048. n.a. means the number is not available as the corresponding dataset was not calculated. A '$-$' means no deglitching is possible as there are only 2 sub-ramps available.

Type	Cyclotron environment		L2 environment	
	1/4s	1/8s	1/4s	1/8s
Raw	89.6	87.3	78.7	76.0
Average over 4	57.2	37.9	59.9	36.7
Average over 8	41.4	(36.2)	41.3	(30.7)
Average over 16	(36.2)	–	(29.6)	–
Raw	n.a.	n.a.	89.4	87.8
Average over 4	n.a.	n.a.	68.1	45.6
Average over 8	n.a.	n.a.	47.8	(35.9)
Average over 16	n.a.	n.a.	(34.8)	–
Raw	n.a.	n.a.	n.a	0.33
Average over 4	n.a.	n.a.	n.a	0.41
Average over 8	n.a.	n.a.	n.a	(0.68)
Average over 16	n.a.	n.a.	n.a	–

7. "Data analysis" of the simulated datasets

The simulated ramps are "analysed" in the following way:

- Glitch positions are determined in the ON- and OFF-source pixel with the appropriate threshold parameter for the glitch finding algorithm.
- Slopes are fitted to unaffected data.

  In other words, no attempt is made to correct for the glitch, and the data after the glitch are not used in the fitting.
- The MEDIAN and STDDEV in all the ON and OFF Slopes is determined.

  Slopes deviating by more than 1.8 sigma from the mean are discarded.
- Following the current AOT design there are 2 ramps per chopper plateau (nChop=2)

  Slopes are median filtered per chopper plateau (which actually means in JIDE taking the average in the case of 2 ramps per chopper plateau)
- For the OFF-pixel, the median Slope per chopper plateau is plotted against total time of the simulation, and a linear fit is made, allowing two rounds of 3 sigma-clipping on the residual. This is a simple way to "monitor responsivity". The total time of the simulation is used here with the idea that the responsivity will be monitored on a timescale longer than the execution of the AOT, e.g. on the timescale of an operational day.

  -This gives the *offset* between consecutive ONs and OFFs
- The signal is constructed: As the input ON-source flux is a fraction of the background, we *divide* ONs and OFFs, rather than subtract: *signal* = ChopON[i] / (ChopOFF[i+1]-*offset*)
- Consider $nON - OFF$= 16 or 192 consecutive *signal*s. Outliers are removed by 2 rounds of 2.6 and 2.8 sigma clipping. The MEAN, MEDIAN and STDDEV and hence the S/N (= MEDIAN/ [STDDEV/$\sqrt{\mathrm{nON - OFF}}$]) are determined.
- As a large dataset is generated, several realisations of this procedure can be generated.

8. Results

The results of the simulations are tabulated in Table 2.

Per "configuration" there are 4 columns, listing the median (minimum - maximum) S/N over the different realisations for ramps of 1/4s (first 2 columns) and 1/8s (last two coloumns), when avaraged over 192 and 16 chopper plateaus (with 2 ramps per chooper platau unless otherwise noted).

The S/N are listed for raw ramps, and when averaged over 4, 8, 16 NDRs, and when slope fitting is employed (w/o deglitching).

A negative S/N means that the best estimate of the source + background flux was **less** than the background flux.

The "configurations" calculated are: (a) for the low-stress module the two radiation environments for a source flux of 1/60 and 1/15 of the background, and (b) for the high-stress module the L2 radiation environments for a source flux of 1/15 of the background, and two special models with 3 ramps per chopper plateau, and very small glitches, respectively.

Figure 3 shows for models (Low-stress module, L2 environment, flux of 1/15th of the background and with 8 sub-ramps [ramps of 32 NDRs and averaging over 4 in the top panel, and ramps of 64 NDRs and averaging over 8 in the bottom panel]) how the S/N varies as a function of the different realisations for a given dataset. The input flux is drawn at a level 1 + 1/15 = 1.0667.

The signal-to-noise behaves approximately as:

$$\text{S/N} \sim \sqrt{\text{ramplength}}\ \sqrt{\text{number\_of\_ramps}}\ \ \text{Signal}$$

The dependence on ramplength and number_of_ramps is as expected, the linear dependence on the strength of the signal is not, and indicates that the noise is dominated by detector noise (and possibly some effect of glitches).

Only in a few cases is onboard slope fitting an option, mainly in the case of 1/8s ramps and when compared to averaging over 16 samples. Both cases suffer from the fact that there is no deglitching, but the slope fitted to all readouts of the raw ramps is more stable than the slope derived from a fit to 2 points.

The S/N significantly drops when averaging over 16 NDRs is used. The improvement of averaging over 8, 4 or raw ramps is much less. This drop in S/N is not only so in the mean but the scatter among the different realisations (as measured by the minimum and maximum S/N among the realisations) also increases strongly.

One way to improve this is to use 3 ramps per chopper plateau instead of 2. The improvement in S/N is much more than a factor of $\sqrt{1.5}$ as the median filter now works effectively, but also the difference between minimum and maximum S/N becomes smaller. In the current simulation, increasing nChop from 2 to 3 leads to better and more stable results than executing the "observation" 2 times.

Table 3 lists the estimated telescope background seen as a point source in the sky taken from Poglitsch instrument model. From table 2 we see that in SED mode we can achieve a S/N of order 12 (say at 80 μm) to 7 (say at 170 μm) in 4 sec of on-source integration time [when averages over 8 samples are available] on a source of 180 (at 80 μm) to 250 (at 170 μm) Jy. This translates into a sensitivity of about 30 and 70 Jy respectively, for a S/N= 1 in 1 sec (**taking the linear dependence of S/N on source flux that is found here.**)

Figure 1 of the GUESSTIMATOR manual lists the flux density in which a S/N of 1 is reached in 1 second and this is about 2.5 Jy at both 80 and 170 μm.

It is concluded that the original sensitivities that went into the GUESSTIMATOR are too optimistic by an order of magnitude when considering the effect of the noise on the ramps, glitches, and the effect of averaging by the OBSW. A comparison with HSPOT is not possible as version 1.6.2 has no SED mode available and it is also explicitly said not to use it as a time estimator for the moment.

The current results are in fact not too surprising when considering the S/N determination in the pre-beam data of the April and October 2005 LLN irradiation tests. There, for ramps of 1/8s, one typically obtained a S/N of 1000 using 256 ramps.

This translates into a S/N of 350 for 32 ramps as applicable in SED mode observations. For a background equivalent of 3000 Jy this would result in an error bar of 8.5 Jy. Observing a source 1/15 of the background implies a total source + background flux of 3200 $\pm$ 9.1 Jy. The source flux would then be determined to be 200 $\pm$ 12 Jy, or be observed with a S/N of 17.

This is the optimistic case as no glitches or responsivity drifts are involved, but is consistent with the S/N values derived from the simulations.

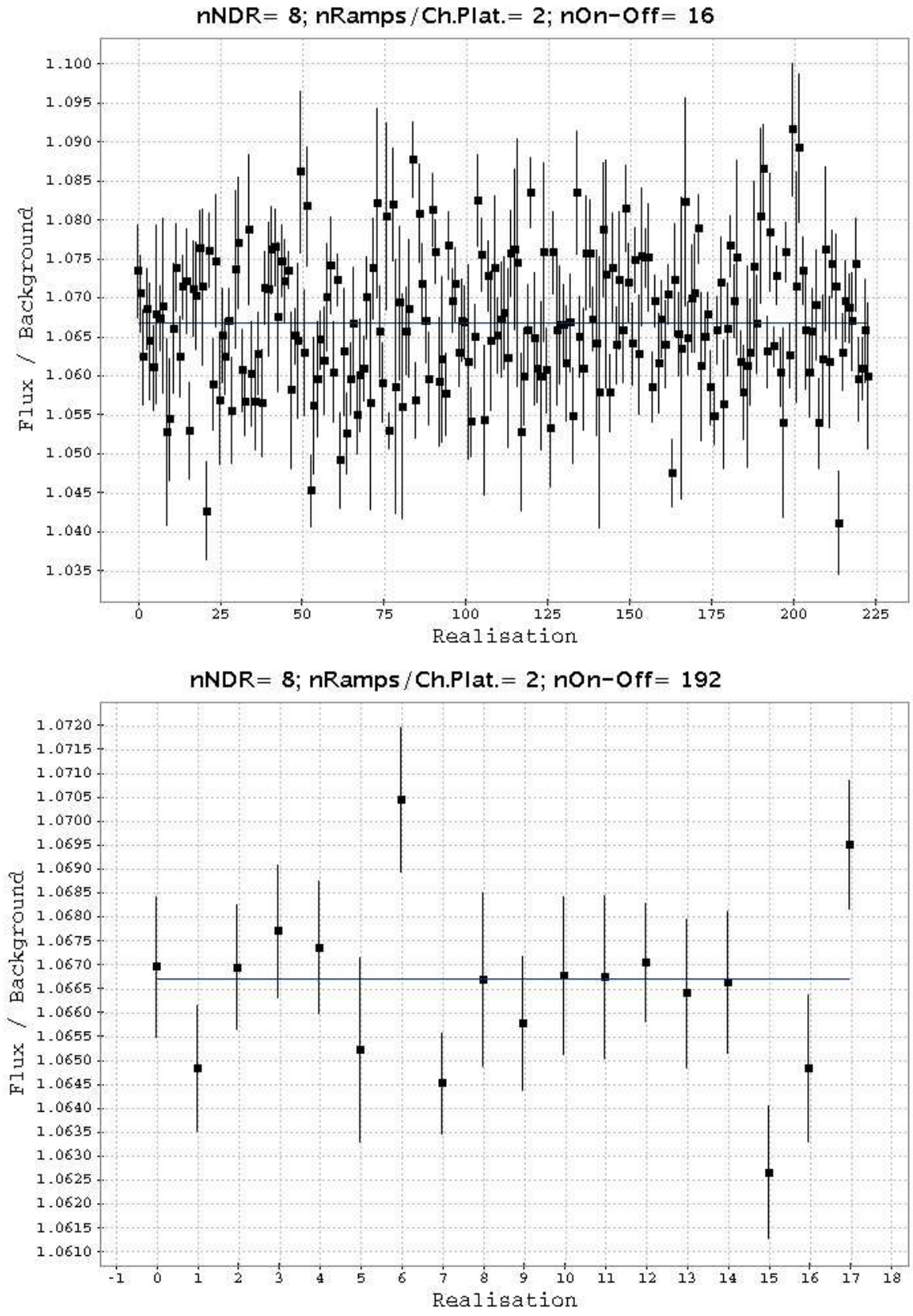

Figure 3: Two examples how the S/N varies as a function of the different realisations for a given dataset. The input flux is drawn at a level 1 + 1/15 = 1.0667.

Table 3: Telescope background flux and equivalent point source in the sky (from AlPog instrument model calculations).

Wavelength (μm)	Flux (W/m^2)	Flux (Jy)
55	4.9 (-14)	2950
60	3.7 (-14)	3000
70	1.8 (-14)	2820
80	3.2 (-14)	2670
100	1.2 (-14)	2260
120	3.2 (-14)	2560
160	2.2 (-14)	3770
200	2.4 (-14)	8600

9. Conclusions

Several datasets have been generated for the PACS spectrometer that take into account the noise properties of the low- and high-stress detectors as observed in pre-beam data during the irradiation tests at Louvain-La-Neuve, as well as educated guesses of the irradiation environment, and are based on current thoughts on AOT design.

Effect of transients, flat-field corrections, data loss because of incomplete grating and chopper movements, and responsivity jumps are not considered, that would tend to lower the S/N derived.

On the other hand the "data reduction" employed is rather basic as it is straightforward and improvement here would lead to a better S/N. This would mean however that we would need to be able to make better use of redundant information, which can not be guaranteed right now, and therefore a conservative approach is warranted.

The conclusions are:

- The signal-to-noise behaves approximately as

  $\mathrm{S/N} \sim \sqrt{\mathrm{ramplength}}\ \sqrt{\mathrm{number\_of\_ramps}}\ \ \mathrm{Signal}$

  The dependence on ramplength and number_of_ramps is as expected, the linear dependence on the strength of the signal is not, and indicates the noise is dominated by detector noise.

- Only in few cases is onboard slope fitting an option, mainly in the case of $1/8s$ ramps and compared to averaging over 16 samples. Both cases suffer from the fact that there is no deglitching, but the slope fitted to all readouts of the raw ramps is more stable than the slope derived from a fit to 2 points.

  Overall however, it is justifiable to work with averages over sub-ramps as this gives a larger flexibility.

- For the OBSW to be able to average 8 samples is imperative.

- 3–instead of 2–ramps/chopper plateau are recommended overall, and are imperative if averages over 16 are to be taken.

- It is concluded that the original sensitivities that went into the GUESSTIMATOR are too optimistic by an order of magnitude when considering the effect of the noise on the ramps, glitches, and the effect of averaging by the OBSW.

Appendix

PR Q-test algorithm is based on the statistical properties of the differential ramps (s[i+1]-s[i]) and (s[i+2]-s[i]) and therefore can not be applied if only few sub-ramps are available.

To be able to detect the largest glitches also in this case, a very simple edge detection algorithm is employed, which has 2 parameters, t1 and t2 (both are positive numbers)

- Construct the differential: Diff[i]= Volt[i+1] - Volt[i]
- Compute the median and standard deviation over Diff, and then edge[i]= (Diff[i] - MEDIAN(Diff))/ StdDev(Diff)
- if edge[j] $<$ -t1 there is a potential glitch, and the glitch height is estimated from
  jump= Volt[j] - (Volt[j-1]+MEDIAN(Diff))
- if jump $>$ t2 then there is a glitch

Like for the Q-test the parameters have been determined to lead to 2% false detection or less.

Table 2: S/N values: median (min-max)

Type	192 ON-OFF	16 ON-OFF	192 ON-OFF	16 ON-OFF
	1/4s ramps		1/8s ramps	
Flux = 1/60 BG; L2 irradiation; Low-stress module				
Raw	12.16 (7.69 - 15.08)	4.03 (0.66 - 13.59)	-	-
Average over 4	11.12 (8.34 - 17.02)	3.67 (-0.74 - 15.24)	-	-
Average over 8	12.83 (8.75 - 15.13)	3.38 (0.05 - 15.32)	-	-
Average over 16	8.63 (5.80 - 11.80)	2.30 (-1.11 - 22.07)	-	-
Slopes	3.35 (1.88 - 04.56)	1.11 (-2.50 - 5.70)	-	-
Flux = 1/15 BG; L2 irradiation; Low-stress module				
Raw	45.74 (24.17 - 68.76)	17.26 (2.94 - 42.20)	38.61 (33.93 - 49.16)	12.04 (3.88 - 33.72)
Average over 4	50.01 (34.36 - 68.05)	14.16 (4.59 - 74.65)	34.51 (28.09 - 45.67)	10.58 (3.26 - 29.95)
Average over 8	45.94 (33.67 - 60.89)	13.23 (3.97 - 54.15)	38.82 (28.60 - 51.37)	12.04 (1.38 - 34.18)
Average over 16	32.70 (21.35 - 45.67)	9.36 (1.57 - 56.87)	6.69 (05.40 - 08.38)	1.90 (-0.84 - 16.24)
Slopes	13.50 (10.95 - 16.61)	4.02 (-0.42 - 16.19)	15.69 (13.39 - 20.00)	4.23 (0.55 - 24.20)
Flux = 1/60 BG; Cyclotron; Low-stress module				
Raw	37.83 (22.57 - 46.42)	11.03 (3.92 - 38.35)	28.58 (18.03 - 41.59)	8.43 (0.83 - 24.32)
Average over 4	38.85 (22.09 - 52.72)	10.92 (3.58 - 31.68)	29.61 (16.92 - 40.14)	8.22 (0.40 - 25.37)
Average over 8	34.52 (21.89 - 45.42)	10.98 (0.05 - 27.54)	25.30 (16.72 - 35.77)	7.32 (0.03 - 18.15)
Average over 16	20.48 (00.32 - 29.17)	07.14 (0.04 - 18.72)	16.88 (10.97 - 28.52)	6.83 (0.47 - 16.37)
Slopes	39.64 (16.96 - 57.22)	11.28 (1.37 - 39.52)	28.30 (16.28 - 42.34)	8.23 (0.53 - 26.39)
Flux = 1/15 BG; Cyclotron; Low-stress module				
Raw	149.45 (91.86 - 178.43)	41.95 (19.75 - 099.29)	93.75 (52.15 - 117.05)	27.08 (12.12 - 86.55)
Average over 4	149.45 (89.06 - 180.35)	41.14 (17.33 - 102.23)	91.19 (52.00 - 116.28)	26.64 (10.32 - 90.14)
Average over 8	129.14 (70.35 - 165.15)	40.66 (00.28 - 100.31)	88.77 (50.22 - 113.08)	26.84 (10.99 - 87.63)
Average over 16	72.18 (01.43 - 103.88)	26.73 (00.19 - 056.74)	69.93 (36.38 - 094.41)	22.69 (01.61 - 55.25)
Slopes	146.90 (61.09 - 197.66)	43.12 (04.22 - 109.93)	87.85 (49.77 - 116.81)	26.43 (07.89 - 86.55)
Flux = 1/15 BG; L2 irradiation; High-stress module; nChop=2; CF=0.48				
Raw	23.94 (12.14 - 37.33)	9.82 (0.96 - 26.01)	21.38 (14.47 - 25.51)	7.32 (2.14 - 23.73)
Average over 4	24.29 (14.51 - 35.78)	8.69 (1.22 - 40.89)	18.98 (11.93 - 23.13)	6.63 (1.09 - 20.71)
Average over 8	17.00 (10.58 - 26.73)	5.86 (0.32 - 45.60)	19.69 (11.27 - 28.31)	7.34 (0.62 - 23.42)
Average over 16	07.83 (03.92 - 14.10)	2.60 (-1.89 - 41.05)	01.95 (01.41 - 02.61)	0.56 (-3.88 - 05.70)
Slopes	03.09 (02.60 - 04.18)	0.99 (-2.56 - 08.05)	03.89 (02.99 - 04.78)	1.22 (-3.13 - 22.80)
Flux = 1/15 BG; L2 irradiation; High-stress module; nChop=3; CF=0.48				
Raw	56.93 (49.62 - 62.02)	16.69 (8.61 - 36.57)	30.37 (27.43 - 34.48)	9.02 (3.73 - 21.87)
Average over 4	50.54 (44.35 - 58.06)	15.72 (4.78 - 28.65)	29.59 (25.80 - 32.92)	8.68 (4.98 - 16.79)
Average over 8	48.48 (44.02 - 55.25)	14.71 (6.53 - 39.92)	30.55 (27.13 - 33.61)	8.66 (4.76 - 22.29)
Average over 16	49.01 (45.62 - 55.70)	15.97 (1.73 - 31.16)	08.38 (05.32 - 15.80)	5.39 (0.34 - 15.19)
Slopes	08.11 (04.96 - 15.17)	03.15 (0.59 - 26.39)	27.27 (25.40 - 31.42)	8.46 (1.97 - 18.03)
Flux = 1/15 BG; L2 irradiation; High-stress module; nChop=2; CF=0.0048				
Raw	–	–	32.20 (29.35 - 38.01)	9.81 (5.08 - 19.26)
Average over 4	–	–	34.12 (28.25 - 40.29)	9.94 (3.89 - 26.00)
Average over 8	–	–	32.51 (27.02 - 37.59)	9.61 (3.77 - 33.05)
Average over 16	–	–	29.03 (26.00 - 33.34)	8.61 (3.84 - 16.64)
Slopes	–	–	33.39 (30.28 - 42.19)	10.07 (5.35 - 27.37)